Anal. Chem. **1999,** *71,* 5340−5347

Quantitative Analysis of Molecular Interaction in a Microfluidic Channel: The T-Sensor

Andrew Evan Kamholz,*,† Bernhard H. Weigl,†,‡ Bruce A. Finlayson,§ and Paul Yager||

Department of Bioengineering and Department of Chemical Engineering, University of Washington, Seattle Washington 98195

The T-sensor is a recently developed microfluidic chemical measurement device that exploits the low Reynolds number flow conditions in microfabricated channels. The interdiffusion and resulting chemical interaction of components from two or more input fluid streams can be monitored optically, allowing measurement of analyte concentrations on a continuous basis. In a simple form of T-sensor, the concentration of a target analyte is determined by measuring fluorescence intensity in a region where the analyte and a fluorescent indicator have interdiffused. An analytical model has been developed that predicts device behavior from the diffusion coefficients of the analyte, indicator, and analyte−indicator complex and from the kinetics of the complex formation. Diffusion coefficients depend on the local viscosity which, in turn, depends on local concentrations of all analytes. These relationships, as well as reaction equilibria, are often unknown. A rapid method for determining these unknown parameters by interpreting T-sensor experiments through the model is presented.

Microfluidics is becoming a prevalent tool for a broad range of applications that include cell separations,[1] flow injection reaction analysis,[2,3] cell patterning,[4] DNA analysis,[5] and cell manipulation.[6] The T-sensor is a microfabricated fluidic device that, due to its small dimensions and typically low volumetric flow rate, is generally operated at Reynolds numbers of less than 1.[7] Inspired in part by the concept of field-flow fractionation,[8] its simplest embodiment (Figure 1a) involves two fluids entering through separate inlet ports and merging to flow adjacently. The microscale conditions induce laminar flow, meaning that there is no convective mixing across the two input streams. Thus, small molecules that can diffuse significant distances during the average residence time of the device will redistribute between streams (Figure 1b). Large molecules or particles that do not diffuse significantly during the same interval will not move appreciably from their original stream unless an external field is applied (such as gravity or an electric field). The critical dimension that governs the extent of

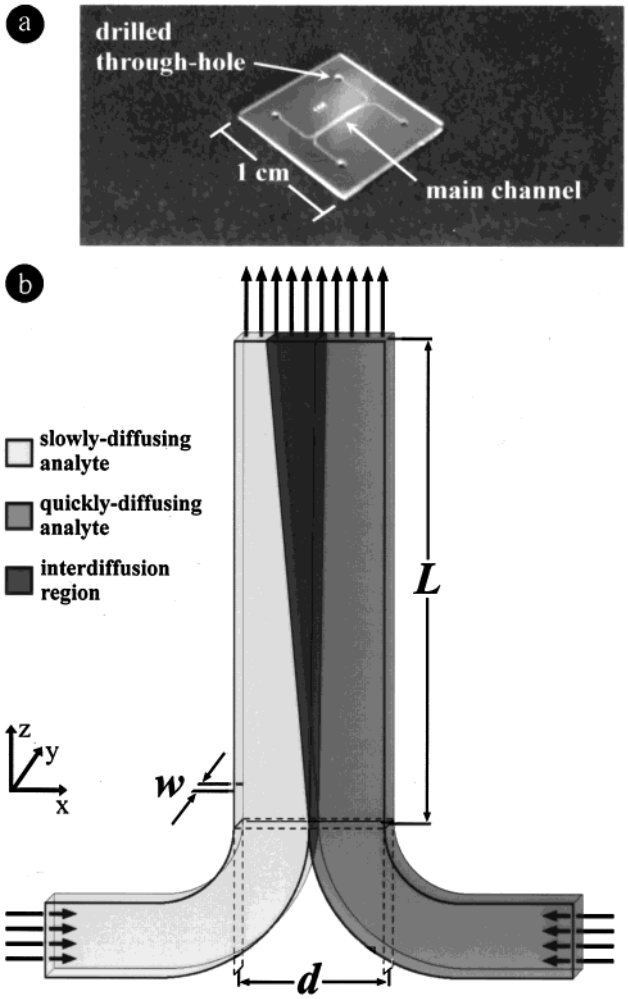

Figure 1. (a) Photograph of a silicon microfabricated device. For operation as a T-sensor, two inputs and one output are used. Both outputs are active when the device is used as an H-filter.[33] (b) Schematic representation of flow in the T-sensor with two input fluids, each containing one diffusing species. The flow is steady state, projecting the interdiffusion along the length of the channel. The asymmetric development of the interdiffusion region (relative to the center of the channel at $^1/_2d$) is due to the difference in diffusion coefficients between the two diffusing species.

* Corresponding author: (e-mail) kamholz@u.washington.edu; (fax) (206) 616 1984.

† Department of Bioengineering, Box 352141.

‡ Present address: Micronics, Inc., 8717 148th Ave. NE, Redmond WA 98052.

§ Department of Chemical Engineering, Box 351750.

|| Department of Bioengineering, Box 352255.

(1) Yang, J.; Huang, Y.; Wang, X. B.; Becker, F. F.; Gascoyne, P. R. *Anal. Chem.* **1999**, *71*, 911−8.

(2) Hodder, P. S.; Blankenstein, G.; Ruzicka, J. *Analyst* **1997**, *122*, 883−7.

(3) Bökenkamp, D.; Desai, A.; Yang, X.; Tai, Y.; Marzluff, E.; Mayo, S. *Anal. Chem.* **1998**, *70*, 232−6.

(4) Kenis, P. J.; Ismagilov, R. F.; Whitesides, G. M. *Science* **1999**, *285*, 83−5.

(5) Simpson, P. C.; Roach, D.; Woolley, A. T.; Thorsen, T.; Johnston, R.; Sensabaugh, G. F.; Mathies, R. A. *Proc. Natl. Acad. Sci. U.S.A.* **1998**, *95*, 2256−61.

(6) Li, P. C.; Harrison, D. J. *Anal. Chem.* **1997**, *69*, 1564−8.

(7) Weigl, B. H.; Holl, M. R.; Schutte, D.; Brody, J. P.; Yager, P. Analytical Methods and Instrumentation, MicroTAS 96 special edition, 1996.

(8) Giddings, J. C. *Science* **1993**, *260*, 1456−65.

10.1021/ac990504j CCC: $18.00
Published on Web 10/28/1999

interdiffusion is the diffusion dimension, d, along which diffusion occurs between streams. The mean residence time is fixed by the value of d, as well as the channel length L, the channel width w, and the input flow rates.[9]

Changes in color or fluorescence of the streams as they progress down the T-sensor can be correlated with physical or chemical properties of the flow system. Some recent examples include monitoring sample pH,[10] viscosity,[11] and fluorescent species.[12,13] With the addition of electrodes in the channel, the T-sensor has also been used to measure concentrations of electrochemically active molecules[14] and perform electrophoretic separation and concentration.[15] A review of developments in T-sensor technology was recently published.[16] Work published to date has generally reported qualitative comparisons between concentrations of analytes in order to determine unknown values. The work presented here demonstrates a method for making direct quantitative measurements with the T-sensor by coupling experimental data to relevant aspects of flow and chemical phenomena in an analytical model.

Low Reynolds Number Flow Theory. The cross section of the T-sensor channel, which in silicon microfabricated devices is usually trapezoidal, can be approximated by a rectangular slot, for which the Reynolds number can be expressed by[17]

$$Re = \frac{\rho(4(A/P))\bar{\nu}}{\mu} \tag{1}$$

where ρ is fluid density, A is device cross-sectional area, P is wetted perimeter, $\bar{\nu}$ is average velocity, and μ is absolute viscosity and with the expression $4(A/P)$ referred to as the hydrodynamic radius. Previous studies have demonstrated that fully developed single-viscosity flow in a rectangular duct with aspect ratio greater than 1 yields a velocity profile that is parabolic over the shorter dimension and approaching plug flow over the longer dimension.[7,18]

The entrance length required for full development of the flow in a circular pipe can be expressed by[19]

$$L_e = D(0.379e^{-0.148Re} + 0.0550Re + 0.260) \tag{2}$$

where L_e is the required length to reach 99% of the fully developed velocity profile and D is pipe diameter. Although the T-sensor geometry is not circular, it is possible to estimate the order of magnitude of the entrance length if the Reynolds number is known.

If the T-sensor inputs are two fluids of different viscosities at the same volumetric flow rate, the dividing line between the two streams will not be down the channel midline. The velocity profile will adjust so that more of the diffusion dimension, d, is occupied by the more viscous fluid, which therefore moves with a slower mean velocity. If the increased viscosity is due to the presence of a diffusable molecule, such as a protein, the local viscosity across d will change as the flow proceeds along the channel and the molecules diffuse down their concentration gradients. As a consequence, the velocity profile will also change as a function of time.

This phenomenon can be used to measure the viscosity of a sample by running it in a T-sensor alongside a fluid of known viscosity. The addition of a dilute fluorophore to one stream allows visualization of the dividing line between streams. If the measurement is made downstream from L_e but before significant interdiffusion has occurred, the following approximation can be applied:[11]

$$\nu_A/\nu_B \approx \mu_A/\mu_B \tag{3}$$

where ν_A is the fraction of the channel occupied by fluid A and ν_B is the fraction occupied by fluid B. This relation falls out of the flow equations assuming that the pressure across the d dimension is uniform at any distance downstream. Since the volume fractions can be measured and one viscosity is known, the other viscosity can be calculated.

Einstein demonstrated that[20]

$$D = RT/f N_A \tag{4}$$

where D is the diffusion coefficient, R is the universal gas constant, T is temperature, and N_A is Avogadro's number. The friction factor, f, is a function of the Stokes radius of the molecule and its aspect ratio and is directly proportional to the absolute viscosity, μ. If environmental factors remain constant such that the extent of hydration and conformation of the molecule do not change, then the friction factor can be expressed as the product of μ and a constant:

$$D = [RT/C_f N_A](1/\mu) \tag{5}$$

where C_f is the proportionality constant between the friction factor and the viscosity. For a given experiment, if the assumptions can be made that temperature and fluid density are constant, then this expression simplifies to

$$D = (c/\mu) \tag{6}$$

where C is a single constant incorporating all factors. Then, if a single value for the diffusion coefficient at a certain viscosity is

(9) Holl, M. R.; Galambos, P.; Forster, F. K.; Brody, J. P.; Afromowitz, M. A.; Yager, P. Proceedings of 1996 ASME Meeting, 1996.
(10) Galambos, P.; Forster, F. K.; Weigl, B. H. Transducers 97, Category 5-Chemical Sensors, 1997.
(11) Galambos, P. Doctoral dissertation, University of Washington, 1998.
(12) Weigl, B. H.; Yager, P. *Sens. Actuators B* **1997**, *38*−*39*, 452−7.
(13) Weigl, B.; Kriebel, J.; Mayes, K.; Yager, P.; Wu, C.; Holl, M.; Kenny, M.; Zebert, D. Proceedings of MicroTAS 98, Banff, Canada, 1998; 81−4.
(14) Darling, R. B.; Yager, P.; Weigl, B.; Kriebel, J.; Mayes, K. Proceedings of MicroTAS 98, Banff, Canada, 1998; 105−8.
(15) Yager, P.; Bell, D.; Brody, J. P.; Qin, D.; Cabrera, C.; Kamholz, A. E.; Weigl, B. Proceedings of MicroTAS 98, Banff, Canada, 1998; 207−12.
(16) Weigl, B.; Yager, P. *Science* **1999**, *283*, 346−7.
(17) Roberson, J. A.; Crowe, C. T. *Engineering Fluid Mechanics*, 5th ed.; Wiley: New York, 1993.
(18) Happel, J.; Brenner, H. *Low Reynolds Number Hydrodynamics*, 2nd rev. ed.; Noordhoff International Publishing: Leiden, 1973.
(19) Dombrowski, N.; Foumeny, E. A.; Ookawara, S.; Riza, A. *Can. J. Chem. Eng.* **1993**, *71*, 472−6.
(20) Einstein, A. *Investigations on the Theory of the Brownian Movement*; Dover Publications: New York, 1956.

known, the value of the constant C can be calculated and the diffusion coefficient can be expressed at any other viscosity.

EXPERIMENTAL SECTION

Device Fabrication. Silicon devices were manufactured using the Washington Technology Center microfabrication facility on the University of Washington campus. Several device variations, all included on a single mask design, were produced by photolithography, described in detail elsewhere.[21] Briefly, test-grade 3-in. silicon wafers (International Wafer Service, Portola Valley, CA) were oxidized in a furnace to a depth of several thousand angstroms. Photoresist (AZ1512, Clariant Corp., Somerville, NJ) was spin-coated, heat-cured, and selectively exposed to ultraviolet light using a quartz mask. The depolymerized photoresist was removed after developing, allowing the exposed oxide layer to be etched with hydrofluoric acid. After the remaining resist was dissolved, the silicon itself was chemically wet-etched where the oxide layer had been removed using ethylenediamine pyrocatechol and water (EPW). Through-holes were drilled with a diamond bit (TSI Inc., Seattle, WA) in a rotary tool (Dremel, Racine, WI). The device was enclosed by anodically bonding a Pyrex glass wafer (U.S. Precision Glass, Elgin, IL) to the silicon. A single wafer was diced into 12 separate devices.

Fluidics. Fluids were delivered using precision syringe pumps (Kloehn Co. Ltd., Las Vegas, NV) outfitted with 50-μL syringes on each of the two input streams. All tubing, valves, and fittings were made from polyetheretherketone (Upchurch Scientific, Oak Harbor, WA), a rigid polymer. Fluid delivery lines were brought in direct contact with the through-holes on the backside of the device. This was achieved by using a custom-built aluminum manifold, which uses screw-down compression fittings to hold the tubing flush against the device. Device design is completely flexible within the limitation that the locations of the through-holes match up with the tubing alignment of the manifold. The syringe pumps are able to provide a much greater pressure than that encountered in the device, allowing for the possibility of using much longer channels for the study of slower processes. The pumps were controlled by a PC using communications software.

All experiments were done in a device with $d = 550$ μm and $w = 25$ μm, an aspect ratio of 22. The buffer viscosity, measured using the T-sensor method described later, was 1.023 ± 0.003 cP and density estimated to be 1.00 g/cm^3. The typical flow rate, determined by the dispense rate of the syringe pumps, was 83.3 nL/s. Approximating the device cross section as a rectangular duct, the Reynolds number calculated from eq 1 is 0.29, which is clearly in the regime of pure laminar flow. To estimate the entrance length, eq 2 can be modified, substituting twice the hydrodynamic radius for diameter, such that

$$L_e = 2(4(A/P))(0.379e^{-0.148Re} + 0.0550Re + 0.260) \quad (7)$$

This yields an entrance length of 61 μm. Measurements in this study were made 5000 μm from the entrance.

A finite element solution of the fully developed velocity profile for a rectangular duct with an aspect ratio of 22 is shown in Figure 2. In agreement with previous results,[7] the profile is uniform across 90% of the d dimension and parabolic across the w dimension.

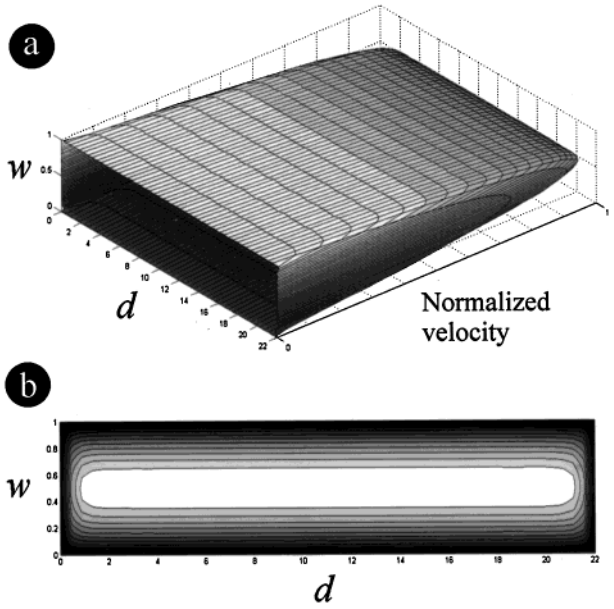

Figure 2. Normalized velocity profile in a microfluidic rectangular duct with aspect ratio (d/w) of 22. The shape of the velocity profile (a) is uniform across the d dimension except near the walls and is parabolic across the w dimension. A contour plot of the velocity in the device cross section (b) demonstrates zero velocity at the walls (black) and uniform maximal velocity in the center (white). Solutions were obtained using a finite element analysis.

Optical Detection. Visualization of the T-sensor was performed using an inverted optical microscope (IM35, Zeiss, Thornwood, NY) operating in epi-illumination. The glass side of the device was placed down on the stage, facing the microscope objective. A 20× objective was used for all measurements. For alignment and focusing, an incandescent light source was used in reflectance mode for bright-field illumination. The desired position for measurement was located and brought into focus. Keeping the device in the same position, the light source was switched to a mercury arc lamp and the filter set was changed to make fluorescence measurements. Fluorescence emission was collected using a three-chip cooled CCD camera (ChromoCam 300, Oncor, Gaithersberg, MD), integrating for 200 frames (6.67 s). Individual integrated frames were captured using a video data acquisition card (CG-7 RGB Frame Grabber, Scion, Frederick, MD) and accompanying software (Scion Image), run on a PC. To account for nonuniformity of the light source, each fluorescence image was divided by a frame taken while the device was flooded with fluorophore.

Albumin and Albumin Blue 580. The molecular system used in this study consisted of human serum albumin (HSA, Sigma A-1653 fraction V, MW $\cong$ 69 000[22,23]) and Albumin Blue 580 (AB580, Molecular Probes A-6663, MW = 306.8), a red fluorophore shown to have high affinity for serum albumins and low affinity for other types of proteins.[24] Native AB580 has a low level of fluorescence, but the quantum efficiency increases by about 2

(21) Brody, J. P.; Kamholz, A. E.; Yager, P. Proceedings of Micro- and Nanofabricated Electrooptical Mechanical Systems for Biomedical and Environmental Applications, San Jose, CA, 1997; 103−10.

(22) Walters, R. R.; Graham, J. F.; Moore, R. M.; Anderson, D. J. *Anal. Biochem.* **1984**, *140*, 190−5.

(23) Maroudas, A. *J. Anat.* **1976**, *122*, 335−47.

(24) Kessler, M. A.; Meinitzer, A.; Wolfbeis, O. S. *Anal. Biochem.* **1997**, *248*, 180−2.

orders of magnitude upon binding to HSA. The nature of this binding event, including the location, number, and affinity of the binding sites, is not reported by the manufacturer or in the current literature. A single molecule of human serum albumin has been shown to bind multiple negatively charged hydrophobic small molecules, each with different kinetics.[25] As AB580 is a small negatively charged hydrophobic molecule, it is reasonable to assume that it also binds to HSA in multiple sites with different kinetics for each. If there are as many as three or four differentiable binding sites per HSA molecule, the equations describing the binding event would be complicated convolutions of exponential processes, even before considering the possible effects of cooperativity or anticooperativity between different sites. Moreover, it is difficult to justify a fit of empirical data with such equations as it is easy to fit any third- or fourth-order exponential equation to most any data set.

Thus, a simplified approach is taken here by assuming that one HSA molecule contains a number, N, of identical binding sites for AB580. These N binding sites are independent and have identical binding kinetics.

$$\text{AB580} + \text{HSAsite} \underset{k_{-1}}{\overset{k_1}{\rightleftharpoons}} \text{complex} \tag{8}$$

where HSAsite is a single binding site on an HSA molecule, complex is a single binding site occupied by an AB580 molecule, k_1 is the rate constant of the forward reaction, and k_{-1} is the rate constant of the reverse reaction. The concentration of HSA binding sites is simply

$$[\text{HSAsite}] = N[\text{HSA}] \tag{9}$$

The equilibrium constant of the AB580/HSA binding event is expressed by

$$K_{eq} = \frac{[\text{complex}]_{eq}}{[\text{HSAsite}]_{eq}[\text{AB580}]_{eq}} \tag{10}$$

The equilibrium concentrations of AB580 and HSAsite are equal to their initial concentrations less the concentration of complex formed.

$$K_{eq} = \frac{[\text{complex}]_{eq}}{(N[\text{HSA}]_i - [\text{complex}]_{eq})([\text{AB580}]_i - [\text{complex}]_{eq})} \tag{11}$$

Solving for the complex concentration yields a quadratic equation.

$$(K_{eq})[\text{complex}]_{eq}^2 - (K_{eq}[\text{AB580}]_i + K_{eq}N[\text{HSA}]_i + 1)[\text{complex}]_{eq} + (K_{eq}[\text{AB580}]_i\, N[\text{HSA}]_i) = 0 \tag{12}$$

Using this expression, it is possible to determine a fit for values of K_{eq} and N by comparing the theoretical results with actual fluorometer measurements.

(25) Curry, S.; Mandelkow, H.; Brick, P.; Franks, N. *Nature Struct. Biol.* **1998**, *5*, 827−35.

All solutions of AB580 and HSA used in this study included 100 mM HEPES buffer, pH 7.5 (Sigma, H-9897), with 0.01% (w/v) BRIJ 35 (Sigma, 430AG-6). The purpose of buffering was to eliminate both any potential pH effects on the quantum efficiency of the dye and pH-related conformational changes of HSA that may have changed its hydration and diffusion characteristics. BRIJ 35 was included to substantially suppress protein adsorption[26] to the silicon and glass surfaces inside the device.

A 1 M stock solution of AB580 was prepared, refrigerated, and used to make all dilutions used in this study. The HSA solutions were made fresh for each experiment. The error associated with concentration values was estimated at 0.5%, based upon the accuracy of the balance used for weighing of reagents.

Fluorometer Measurements. The extent of binding for a range of AB580 and HSA concentrations was determined based on fluorescence measurements made using a fluorometer (LS-50B, Perkin-Elmer, Norwalk, CT) with a short-path-length (5 mm) cuvette. Samples were excited at the AB580 absorption peak of 580 nm. Emission intensity was measured at 606 nm, the emission peak for the complex.

Stopped-Flow Analysis. The forward and reverse rate constants of the AB580−HSA reaction were determined by using a stopped-flow apparatus (SFA-11, Hi-Tech, Salisbury, U.K.). The theory of such experiments is explained in detail elsewhere.[27] Briefly, two reactants are rapidly injected into a cuvette using syringes. During this injection, the contents of the cuvette are mixed but essentially unreacted. When injection ends, which happens abruptly when the syringes reach a physical stop, the contents of the cuvette begin reacting. Thus, if there exists some optical parameter that changes as the reaction proceeds, it can be observed as a function of time from start to finish. From such data, a time constant of the reaction can be estimated.

Stopped-flow analysis is ideal for studying the AB580−HSA binding event due to the significant change in fluorescence that occurs. To monitor the reaction, the cuvette from the stopped-flow apparatus was placed on the microscope stage so that its contents were illuminated from the mercury arc source at 580 nm. One end of a fiber optic was placed at 90° to collect fluorescence emission. The other end was attached to a spectrophotometric data acquisition card (PC1000, Ocean Optics, Dunedin, FL) that recorded real-time spectral intensity at approximately 60 Hz.

Analytical Model. An analytical model was created that describes the T-sensor. The parameter set consisted of device geometry, flow rates, two-dimensional velocity profile, binding reaction between AB580 and HSA, diffusion of AB580, HSA, and the complex, and viscosity effects on the velocity profile and diffusion coefficients. However, is was possible to design T-sensor experiments that justified a number of simplifying assumptions that greatly decreased the run time of the simulation.

First, because of the integration capabilities of the CCD camera, only micromolar concentrations of AB580 and HSA were required to achieve a good signal-to-noise ratio. Using the T-sensor and eq 3, the viscosity of HSA as a function of its concentration was measured (Figure 3). The maximum concentration of HSA used in this study resulted in an increase in viscosity of less than

(26) Towns, J. K.; Regnier, F. E. *Anal. Chem.* **1991**, *63*, 1126−32.
(27) Atkins, P. W. *Physical Chemistry*, 6th ed.; Oxford University Press: New York, 1998.

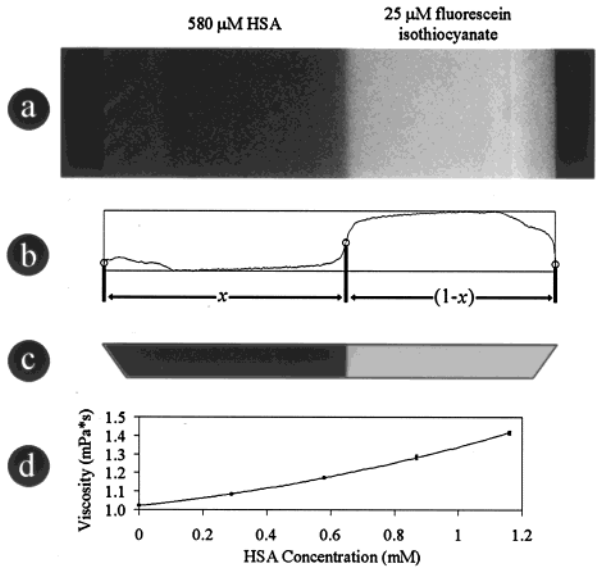

Figure 3. Measurement of viscosity in the T-sensor. The solution of interest, in this case one containing HSA, is introduced alongside buffer containing a trace amount of fluorescein. Both input fluids have the same flow rate. The presence of the fluorophore allows visualization of the interface between the streams (a). A plot of the fluorescence intensity across the channel (b) allows determination of the fraction of the channel occupied by protein (x) and the fraction occupied by buffer ($1 - x$). Consideration of the geometry of the T-sensor (c) allows for calculation of the volume fraction of the channel occupied by each fluid. The viscosity ratio is equal to the voume fraction ratio as in eq 3. Successive experiments allow for calibration of viscosity of HSA as a function of concentration (d). The best fit is $\mu = 1.0233 + 0.1763c + 0.1402c^2$, $R^2 = 0.9999$, where c is concentration and the units are as in the figure. The form of this equation and its physical significance have been discussed elsewhere.[11] Values obtained by this method are consistent with other published measurements of albumin viscosity.[34]

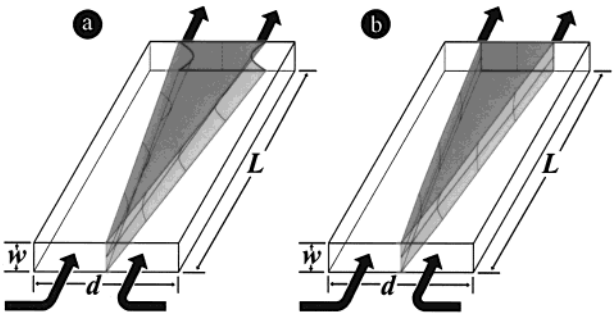

Figure 4. Conceptual rendering of the shape of the interdiffusion region as flow proceeds in the T-sensor. If diffusion only in the d dimension is considered (a), more diffusion will occur near the top and bottom surfaces, where the velocity is slow. This causes the interdiffusion zone to be shaped like a butterfly and should occur in practice when the mean interdiffusion distance across d is significantly less than the width, w. Considering diffusion in both the d and w dimensions (b), there will be equilibration across the width if the mean interdiffusion distance across d is significantly greater than w. This concept is based entirely on the distribution of residence times caused by the nonuniform velocity profile. Additional complications to the shape of the interdiffusion zone arise when the possibility of wall interactions is considered.

0.2% relative to the buffer. Thus, it is justified to assume that all solutions used in this study have the same viscosity, equal to that of the buffer.

Also, two assumptions arise from the shallow etch depth of the device, which was 25 μm. First is the notion that fluorescence from all fluid along the w axis was collected uniformly. The stage was moved such that the focal plane lay equidistant between the surface of the glass and the bottom of the device (at $^1/_2w$) so that the fluorescence signal was collected as evenly as possible throughout the etch depth.

The other assumption arises from the expected shape of the interdiffusion zone between the two input streams. For a particular device geometry, the mean distance across d that the molecules interdiffuse depends on the flow rates, the distance downstream of the measurement, and the diffusion coefficients of the species of interest. If the resulting mean interdiffusion distance is significantly less than the width, then molecules near the top and bottom of the device would interdiffuse significantly further because of the longer residence time in these regions of the channel (Figure 4a), resulting in the "butterfly effect". However, when the mean interdiffusion distance has increased beyond the value of w, the molecules will also have diffused throughout the w dimension, moving between the slower moving and faster moving laminae during this time (Figure 4b). As long as the observed interdiffusion distance is significantly greater than w, it is justifiable to assume that the contents of the channel are uniform throughout w. As shown in later data, the interdiffusion distance in this study was approximately 60 μm, allowing application of this assumption.

Although the velocity profile across d is nearly uniform, the wall effects would need to be considered if the interdiffusion distance were at least 90% of d, or about 500 μm. In such a case, the concentration gradients of the diffusable analytes would be affected by the slower moving laminae near the side walls. However, as the interdiffusion distance was only approximately 10% of d, there is no need to consider the velocity profile near these walls.

Applying these assumptions, the velocity can be regarded as constant everywhere in the T-sensor. It should be stressed that this assumption refers only to the distribution of molecules and is valid only with the particular parameters outlined. Thus, the velocity is only a proportionality constant between the time elapsed and the distance traveled down the channel. The general expression for a diffusing, reacting species is[28]

$$V_z\frac{\partial C_n}{\partial z} = \frac{\partial C_n}{\partial t} = D_n\left(\frac{\partial^2 C_n}{\partial x^2}\right) \pm R \qquad (13)$$

where C is concentration, D is diffusion coefficient, R is production or elimination due to binding/unbinding, and $n = 1, 2, 3, ...$, for however many species are present (coordinate axes are as in Figure 1b). For the AB580−HSA reaction, the rate of production of complex is k_1[AB580][HSAsite] while the rate of elimination is k_{-1}[complex]. The overall rate is most conveniently expressed by combining these terms and expressing k_{-1} as the ratio of k_1 and K_{eq} such that

(28) Bird, R.; Stewart, W.; Lightfoot, E. *Transport Phenomena*; John Wiley & Sons: New York, 1960.

$$R = k_1\left([\text{AB580}][\text{HSAsite}] - \frac{[\text{complex}]}{K_{eq}}\right) \qquad (14)$$

This term must be negative for the rates of change of concentration of AB580 and HSA but positive for the complex. The full system of equations is then

$$\frac{\partial[\text{AB580}]}{\partial t} = D_{\text{AB580}}\left(\frac{\partial^2[\text{AB580}]}{\partial x^2}\right) - k_1\left([\text{AB580}][\text{HSAsite}] - \frac{[\text{complex}]}{K_{eq}}\right) \qquad (15a)$$

$$\frac{\partial[\text{HSAsite}]}{\partial t} = D_{\text{HSA}}\left(\frac{\partial^2[\text{HSAsite}]}{\partial x^2}\right) - k_1\left([\text{AB580}][\text{HSAsite}] - \frac{[\text{complex}]}{K_{eq}}\right) \qquad (15b)$$

$$\frac{\partial[\text{complex}]}{\partial t} = D_{\text{HSA}}\left(\frac{\partial^2[\text{complex}]}{\partial x^2}\right) + k_1\left([\text{AB580}][\text{HSAsite}] - \frac{[\text{complex}]}{K_{eq}}\right) \qquad (15c)$$

One feature of note is that concentration is solved for HSAsite rather than for HSA. The concentration profile for HSA can be recovered after analysis simply by dividing by the number of binding sites per molecule, N. This is generally not necessary since the concentration profiles for only the fluorescent species are needed for the final analysis. Also, the diffusion coefficient of the complex is taken to be the same as the diffusion coefficient of HSA, since HSA is a much larger molecule than AB580. Major conformational changes in HSA that could significantly affect the diffusion coefficient are absent upon binding of fatty acids similar in size and hydrophobicity to AB580.[25]

The system of equations is solved by defining a line of nodes across the diffusion dimension and transforming the system into finite difference expressions. This simple method has been described in detail elsewhere.[29] Briefly, the differential equations are expressed as Taylor expansions, the values of which can be calculated based on the concentration values at each node. The boundary condition prohibits flux at the walls, although the behavior at the walls has no effect on the behavior in the region of interdiffusion within the time course of a typical simulation. Entry length effects are neglected, thereby requiring that actual data are taken from a point well downstream of L_e. The total integration time is defined by the location at which the measurements are made (the distance downstream from the entrance) and the flow rate. The system of finite difference equations was solved by a MATLAB (MathWorks, Natick, MA) ordinary differential equation solver on a PC (Golden International Corp., Seattle, WA). Typical simulations in this study solved a system of 237 nodes and took approximately 2 min using a 200-MHz Pentium processor.

RESULTS AND DISCUSSION

By assuming that the binding event between HSA and AB580 can be characterized by N identical, noncooperative binding sites per HSA molecule, the equilibrium constant was determined from measurements in a fluorometer. The forward and reverse rate constants were determined using stopped-flow technique.

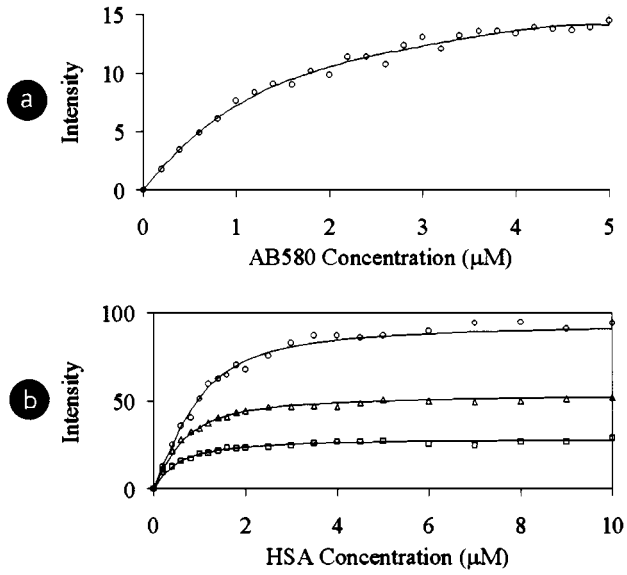

Figure 5. Fluorometer measurements of the fluorescence intensity of native AB580 (a) as a function of concentration. To remain within the linear portion of the curve, starting AB580 concentrations of 1 μM were used. Adding HSA (b) greatly increases the quantum efficieny of AB580. Shown is the fluorescence intensity of solutions containing 0.5 (□), 1.0 (△), and 2.0 μM AB580 (○) over a range of HSA concentrations. Solid lines are analytical fits using $K_{eq} = 1.36 \times 10^6$ M^{-1} and $N = 2$. The best fits were found by minimizing the residuals produced by the three data sets for given values of K_{eq} and N.

Determination of K_{eq}, N, k_1, and k_{-1}. Fluorescence emission intensities as collected in a conventional spectrophotometer for 0.5, 1, and 2 μM AB580 over a range of HSA concentrations up to 10 μM are shown in Figure 5. The short path length and micromolar concentrations allow application of Beer's law, thus assigning direct proportionality between the concentration of the complex and its fluorescence. However, the measured emission intensity is the sum of fluorescence from the complex and from the native dye. Therefore, it was necessary to first characterize the fluorescence of native AB580 (Figure 5a). Then, it was possible to apply corrections to a raw data set of AB580−HSA fluorescence by using the values for K_{eq} and N to determine the amount of native dye present at each data point. The best fit between theoretical data and corrected data (Figure 5b) was determined by minimizing residuals and yielded values of 1.36×10^6 M^{-1} for K_{eq} and $N = 2.0$. This set of experiments also showed that the emission intensity of the native dye is linear with concentration in a 5-mm cell up to 1 μM, which was set as the upper limit for concentration in later T-sensor experiments.

Using 4 μM AB580 and 8 μM HSA as the two input solutions in the stopped-flow apparatus, the time constant of the formation of complex was determined to be 0.0447 ± 0.003 s. For this bimolecular binding event, the time constant (time for reaction to reach 63% of completion) is related to the kinetic parameters by[30]

(29) Finlayson, B. A. *Nonlinear Analysis in Chemical Engineering*; McGraw-Hill: New York, 1980.

(30) Bernhard, S. A. *The Structure and Function of Enzymes*; W. A. Benjamin: New York, 1968.

$$\frac{1}{\tau} = k_1([\text{AB580}] + [\text{HSAsite}]_i) + k_{-1} \qquad (16)$$

Since K_{eq} is the ratio of forward to reverse rate constants, this expression can be manipulated such that

$$k_1 = \frac{1}{\tau([\text{AB580}]_i + [\text{HSAsite}]_i + 1/K_{eq})} \qquad (17)$$

This yields a value of $k_1 = (2.084 \pm 0.023) \times 10^6\ s^{-1}\ M^{-1}$ (the error is cumulative, based upon the intensity resolution of the data acquisition card and the uncertainty of concentration values). Dividing this by K_{eq} yields a value for k_{-1} of $1.529 \pm 0.017\ s^{-1}$. It is important to stress that although this method, which assumes a single population of identical binding sites, is almost certainly not accurate, the analytical solution does accurately predict the concentration of complex formed within the range of concentrations used here. The equilibrium constant and reaction rate constants measured here are certainly good only for the particular type of HSA used. This lot of HSA was not fatty-acid free and therefore there may be competition for AB580 binding sites both from endogenous fatty acids and from the BRIJ 35 added during preparation.

AB580 Diffusion Coefficient Determination. The diffusion coefficient of AB580 was determined in the T-sensor by conducting experiments in which 1 μM AB580 was introduced on the right side of the channel and buffer was introduced on the left. It is advantageous to determine this parameter empirically rather than estimating from the molecular weight so that any effects specific to the T-sensor, such as wall interactions, can be accounted for. Because all fluids used in this study were buffered at the same pH with the same ionic strength, it is reasonable to assume that the value for the AB580 diffusion coefficient found is valid throughout all experiments.

Three trials were conducted at flow rates of 83.3, 416, and 833 nL/s. The effect of increasing the flow rate is to decrease the average residence time and thereby decrease the extent of interdiffusion of the two fluids at a fixed observation point. Data were captured at 5 mm downstream and were normalized by dividing by a set of data taken when the channel was flooded with AB580. Three model simulations were conducted, changing the diffusion coefficient of AB580 until the best collective fit was found. The comparison of actual data to analytical results yields a diffusion coefficient for AB580 of $4.55 \times 10^{-7}\ cm^2/s$ (Figure 6). The diffusion coefficient of sucrose, a molecule of similar molecular weight and shape, has been measured at $4.5 \times 10^{-7}\ cm^2/s$.[31]

Even the best fit of analytical data to the empirical results shows some slight discrepancy, with systematic errors of as much as 5% for some portions of the curve. This is because the actual data do not form a perfectly symmetric sigmoid, while any analytical results using the particular variation of the model discussed here will produce such a sigmoid. The measured effect should not be due to changes in quantum efficiency of the dye since earlier fluorometer measurements demonstrated that 1 μM is within the linear range of fluorescence of AB580. Any changes in local viscosity would affect the local diffusion coefficient, but the dye is so dilute that the viscosity is essentially that of pure buffer everywhere. The most likely explanation is that indicator molecules experience wall interactions and their local diffusion coefficients are significantly slowed when near any wall.

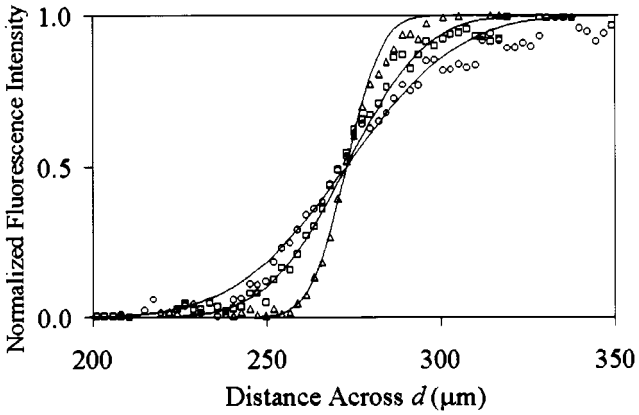

Figure 6. Fluorescence intensity profiles for the distribution of AB580 (with no HSA) across the *d* dimension at a distance of 5000 μm downstream. Flow rates are 83.3 (○), 416 (□), and 833 nL/s (△). Solid lines representing the free diffusion of AB580 are analytical fits using $D = 4.55 \times 10^{-7}\ cm^2/s$.

Validation of Model. T-sensor experiments were conducted using two solutions containing 1 μM AB580 on the right and HSA on the left at concentrations of 0, 2, 4, 6, and 8 μM (Figure 7a). The flow rate for each experiment was 83.3 nL/s, yielding an average interdiffusion time of 0.81 s. Measurements were made at 5 mm downstream from the point at which the streams merge (Figure 7b). Simulations for each experiment were conducted using the kinetic parameters as previously discussed. Modeled curves were fit to experimental data by scaling the distributions of native dye and complex and adding the results to generate total predicted fluorescence. The best fit was determined by finding what value of HSA diffusion coefficient produced the least residual cumulative error for the set of five curves. This best fit between measured and analytical data occurred at a diffusion coefficient for HSA of $1.3 \times 10^{-6}\ cm^2/s$ (Figure 7c). On the basis of accumulated experimental error, including the 8-bit resolution of the camera, this figure is estimated to have 5% uncertainty.

This value for the diffusion coefficient is approximately twice the values found in the literature ($6.43 \times 10^{-7}\ cm^2/s$,[22] $6.1 \times 10^{-7}\ cm^2/s$ [32]). The most likely explanation for this discrepancy is the presence of wall interactions by both the HSA and AB580 molecules.

CONCLUSIONS

Previously, the T-sensor was used qualitatively to estimate the concentration of a target analyte. This study developed the T-sensor as a research tool, employing the combination of experimental data with an analytical model to quantitatively describe molecular interactions in a microchannel. At its simplest level, the model is a design tool that considers device geometry,

(31) Perry, J. H., Ed. *Chemical Engineer's Handbook*, 3rd ed.; McGaw-Hill: New York, 1950.

(32) Sober, H. A., Ed. *Handbook of Biochemistry*, 2nd ed.; CRC Press: Cleveland, 1970.

(33) Brody, J. P.; Yager, P. *Sens. Actuators A* **1997**, *58*, 13−18.

(34) Wetzel, R.; Becker, M.; Behlke, J.; Billwitz, H.; Bohm, S.; Ebert, B.; Hamann, H.; Krumbiegel, J.; Lassmann, G. *Eur. J. Biochem.* **1980,** *104*, 469−78.

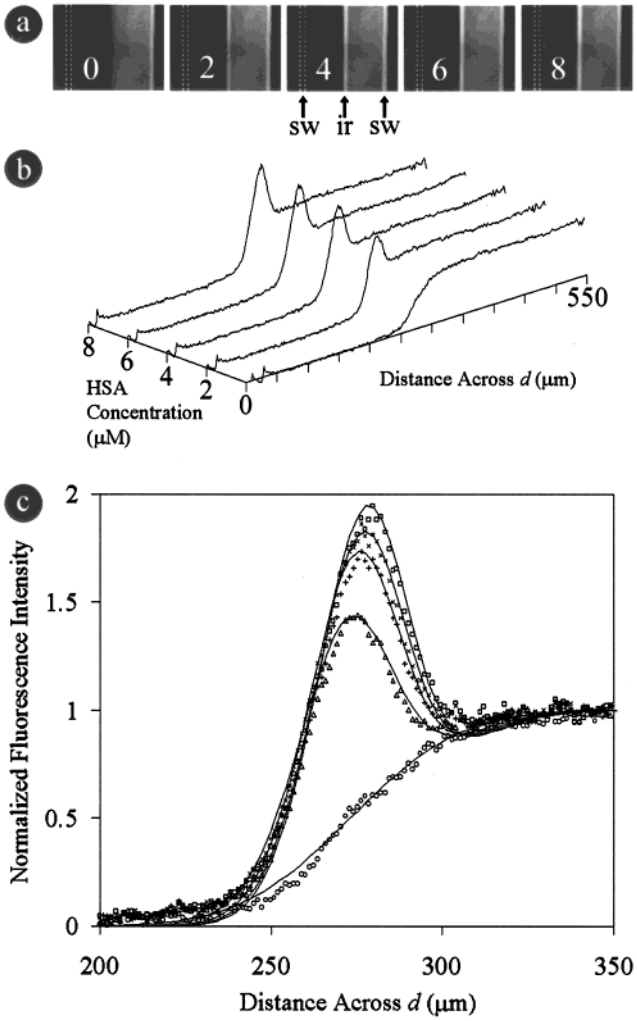

Figure 7. Images of T-sensor experiments (a) with HSA on the left and 1 μM AB580 on the right. Numbers on figures indicate HSA concentrations (in μM). The right side wall (sw) is visible due to reflected fluorescence while the left side wall is not visible. The intensity of the interdiffusion region (ir) is higher with increasing HSA concentration. The fluorescence intensity across d is plotted at a distance of 5 mm downstream (b) for the five different HSA concentrations. The five sets of data (c) are plotted together for HSA concentrations: 0 (○), 2 (△), 4 (+), 6 (×), and 8 μM (□). Solid lines are analytical fits using an HSA diffusion coefficient of 13.0×10^7 cm^2/s.

flow rates, diffusion coefficients, and reaction rates. Even if some of these parameters are unknown, it is possible to estimate the required length of T-sensor to achieve a desired interdiffusion distance given an operable range of flow rates. The more detailed example presented in this work demonstrates a method for using the T-sensor to quantitatively determine molecular properties. The set of properties considered in the model includes diffusion coefficients of both species and their complex and the forward and reverse rate constants; any one unknown can be determined if the others are known.

The T-sensor offers a number of advantages as a microfluidic chemical sensor. Even in a continuous-flow format, sample volumes as little as 1 μL can be used. The interdiffusion events, and thus the measurement time, are very fast, usually occurring in less than 1 s. A particular fluorescent molecule of interest can be studied in any fluid, allowing for the measurement of diffusion coefficient and viscosity dependence on pH, ionic strength, and other environmental factors. In the case of the study shown here, however, the diffusion coefficient of a nonfluorescent protein was measured by using an indicator. Moreover, such T-sensor assays are amenable to the use of absorbance labels and electrochemical detection.[14] In the case of fluorescence, very sensitive detectors such as CCD cameras allow the use of lower concentrations of indicator than many other assay types.

A logical application of the methods described here is the characterization of molecular binding for which the reaction rates are not easily measurable by traditional techniques. A single set of T-sensor experiments that includes the proper controls can be used with the model to determine diffusion coefficients and reaction rate constants. In addition, the device design is highly flexible, allowing for geometries that can accommodate a range of both diffusion speeds and reaction rates. Other systems of interest that could be studied in the T-sensor include protein−protein interactions, immunoassays, and DNA hybridization assays.

The version of the model in this study was two-dimensional; it considered concentrations across the d dimension and developed them down the length of the channel. The results strongly suggest that it is suitable for modeling the primary processes in the T-sensor. However, work subsequent to this study has suggested that molecule−wall interactions may significantly affect the apparent diffusion coefficient. In a device with such a high surface area-to-volume ratio, this is to be expected. Currently, a full three-dimensional model is being prepared that does not employ assumptions about uniformity across the width and allows for adsorption (or other rate-determined interactions) to the walls. It is hoped that this addition, in combination with additional experiments, will elucidate the more complex factors seen in microfluidic devices.

ACKNOWLEDGMENT

This work was supported by the DARPA Contract N660001-97-C-8632 and Micronics, Inc. The stopped-flow apparatus was graciously provided by Professor John Berg, Department of Chemical Engineering, University of Washington. The authors thank the Washington Technology Center, managed by Mr. H. Sho Fuji, and Mr. Gary Holman and Mr. Darrel Bell for fabricating devices. In addition, the authors would like to recognize extensive groundbreaking work on this type of T-sensor experiment designed and performed by Dr. Margaret Kenny, Ms. Diane Zebert, and Mr. Greg Hixson, as well as the team that originally developed the T-sensor, including Dr. James Brody and Dr. Mark Holl. Also greatly appreciated is the continual support of all of the members of the Yager research group, particularly Mr. Anson Hatch, Ms. Catherine Cabrera, Dr. Katerina Macounova, and Mr. Kenneth Hawkins for insightful scientific discussions and Dr. Holl for the majority of the design and implementation of the fluidics system and the aluminum device manifold. Authors P.Y. and B.H.W. have financial interests in Micronics, Inc.

Received for review May 13, 1999. Accepted September 21, 1999.

AC990504J